ELSEVIER

Infrared Physics & Technology 42 (2001) 467–472

INFRARED PHYSICS & TECHNOLOGY

www.elsevier.com/locate/infrared

# High-gain quantum-dot infrared photodetector

V.V. Mitin [a,*], V.I. Pipa [a,b], A.V. Sergeev [a], M. Dutta [c], M. Stroscio [c,1]

[a] Department of Electrical and Computer Engineering, Wayne State University, Detroit, MI 48202, USA

[b] Institute of Semiconductor Physics, Kiev 252650, Ukraine

[c] US Army Research Office, P.O. Box 12211, Research Triangle Park, NJ 27709-2211, USA

**Abstract**

An innovative idea in design of sensitive quantum-dot (QD) infrared photodetector is to use a structure with QDs surrounded by repulsive potential barriers which are created due to interdot doping. Spatial separation of the localized ground state and continuum conducting states of the electron increases significantly the photoelectron capture time and photoconductive gain. Large value of the gain results in high responsivity, which in turn improves detectivity and raises the device operating temperature. © 2001 Elsevier Science B.V. All rights reserved.

*PACS:* 07.57.Kp; 85.60.Gz

*Keywords:* Photodetector; Quantum dot; Potential barrier; Capture

## 1. Introduction

Numerous applications, such as night vision, satellite imaging, medical thermography, and chemical spectroscopy, place stringent requirements on the sensitivity and operating temperature of infrared detectors. State-of-the-art detectors employ narrow bandgap semiconductors, particularly $Hg_{1-x}Cd_xTe$ [1,2], and various quantum well (QW) structures [3,4]. Due to more advanced technologies, the performance of these detectors have been constantly improving. However, the possibilities for further significant improvement of these detectors are almost exhausted. The limitations of narrow-gap materials and QW structures are mainly conditioned by the tremendous decrease in the photocarrier lifetime when approaching room temperature. Therefore, both kinds of detectors require cooling to achieve the responsivity and sensitivity, which are necessary for applications.

For the last several years, the interest has been growing in optoelectronic devices based on zero-dimensional semiconductor nanostructures (quantum dots (QDs)). Self-aggregation of quantum dots (QDs) during the epitaxial deposition of strained semiconductor layers (Stranski–Krastanov growth mode) allows one to fabricate high quality QD superlattice nanostructures [5,6]. Recently, a few groups have investigated possibility of using the self-assembled InAs–GaAs QD array as an infrared photodetector [7–12]. Due to the atom-like localised electronic states, QD infrared

* Corresponding author. Tel.: +1-313-577-8944; fax: +1-313-577-1101.

*E-mail addresses:* mitin@ece6.eng.wayne.edu (V.V. Mitin), stroscio@aro-emh1.army.mil (M. Stroscio).

[1] Also corresponding author. Fax: +1-919-549-4349.

1350-4495/01/$ - see front matter © 2001 Elsevier Science B.V. All rights reserved.
PII: S1350-4495(01)00107-4

photodetectors (QDIPs) ideally have advantages over quantum well photodetectors (QWIPs). QD structures can straightforwardly absorb a normal incident photon flux, and, hence, it is not necessary to use the special optics, gratings, or reflectors as is required for QWIPs which are insensitive to normal incidence photoexcitation. It is also very important that the discreteness of the electron energy spectrum increases substantially the electron capture time and hinders (due to the phonon bottleneck effect [13]) the intradot energy relaxation. According to measurements [14], the capture times in self-assembled QD lasers are 30–50 ps, which exceeds by an order of magnitude the capture times measured for QW lasers [15]. The increase of the capture time improves responsivity of the photodetector.

QDIPs are based on the two different types of carrier photoexcitation: the electron transitions from the ground state of a QD to the excited localized state (bound-to-bound transitions), and transitions from the localized state to the continuum spectrum (bound-to-continuum transitions). In the latter case, the energy of photoexcited electrons may belong to the 3D or to 2D continuum depending on the structure of the QD system. QDIPs with bound-to-bound transitions have been considered in Refs. [7,8,16], bound-to-continuum transitions theoretically in Refs. [17,18]. In Ref. [9] both types of QDIPs were designed and investigated. The typical operating temperature ranges from 10 [16] to 30 K [11], and higher operating temperature, such as 60 [19] and 80 K [9], have been reported. In Ref. [12] photoconductivity was observed up to 190 K, demonstrating the superiority of InAs QDIPs for high-temperature operation. QDIPs show encouraging performance and the initial experiments have already demonstrated significant advantages of QDIP over QWIP. However, at the present time, the design and operating regimes of QDIP are still very far from optimum.

In a self-assembled QD heterostructure one may use such macroscopic parameters as the photoelectron lifetime, $\tau_l$, and the drift velocity, $v_d$. Introducing the drift length, $L_d = v_d\tau_l$, as the distance which an electron traverses during lifetime $\tau_l$, one can express the photoconductive gain as

$$g = L_d/L = \tau_l/\tau_{tr}, \quad (1)$$

where $L$ is the distance between electrodes, and $\tau_{tr} = L/v_d$ is the transit time. If the capture into QDs and ejection from the QDs are the only processes which limit the electron lifetime, the capture time coincides with the photoelectron lifetime $\tau_l$. According to Eq. (1), the short transit time, together with the long capture time, results in a high value for the photoconductive gain, which in turn leads to high responsivity and detectivity.

To make the transit time shorter, it is desirable to have a high mobility of photoelectrons, a large value of the applied electrical field, and a small distance between the contacts. However, a significant decrease of the transit time is unrealistic. In our opinion, the optimal way to improve photoconductive gain is to hinder the photoelectron capture. In the present paper we show that this goal can be achieved in the structures with QDs surrounded by repulsive potential barriers which are created due to interdot doping. In QDIPs with bound-to-continuum transitions, the barriers will separate the ground and excited states and prevent fast capturing of photoelectrons into the dots.

## 2. Barrier-limited photoelectron capture

Electronic parameters of QD structures may be controlled over a wide range by varying the level of intradot doping and changing the characteristic distances associated with the dot structure. We consider a heterostructure consisting of spherical QDs and doped interdot area. Electrons from impurities populate QDs. We assume that $N$ ($N \gg 1$) electrons are localized in each dot, creating a depletion area around the dot. The potential relief is shown in Figs. 1 and 2. The confinement potential $U(r)$ is given by the band-offset, $U_0$. The total electron potential energy is the sum $U(r) + V(r)$, where $V = e\phi$ is the electrostatic energy. The potential $\phi$ is created by electrons bounded in QD and by ionized donors placed outside the dot. We assume that the electron density distribution inside the dot has spherical symmetry and the positive charge of donors is uniformly distributed in a spherical shell $a \leqslant r \leqslant b$,

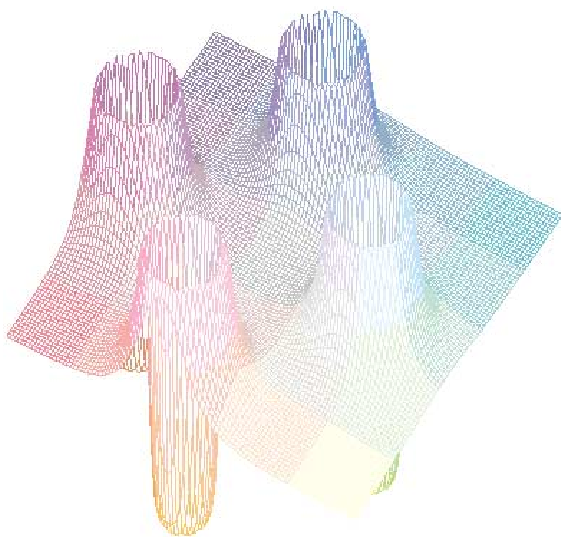

Fig. 1. Potential relief of QD array.

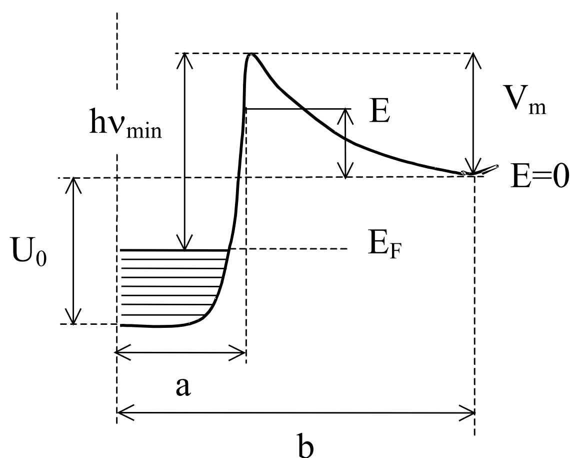


Fig. 2. Energy band diagram in QD plane.

where $a$ is the QD radius, $2b$ is the interdot distance. Number of confined electrons $N$ is determined by the concentration of donors $N_d$ through the electroneutrality condition. The suggested structure may be realized in the traditional self-assembled InAs/GaAs QD array. The potential barriers surrounding QDs are created by doping of GaAs by Si (it is desirable to avoid intradot doping). In Fig. 1 we show the smooth potential, which corresponds to large number of electrons in a QD. At small number of electrons in the QD, the barrier potential loses its spherical symmetry. In this case the potential distribution is very sensitive to the positions of the charged impurities. For large number of electrons in a QD ($N \gg 1$), the quasi-classical approximation can be employed. It allows to estimate the upper value of electron energy of the states occupied by electrons as the Fermi energy

$$E_F = \left(\frac{9\pi N}{4}\right)^{2/3} \frac{\hbar^2}{2ma^2}, \tag{2}$$

where $m$ is the electron effective mass. We consider the QDs with the large band-offset and large ionization energy: $U_0 - E_F \gg kT$, where $k$ is the Boltzmann constant and $T$ is the temperature. In this case the density of the thermoexcited electrons is small and may be neglected in the electroneutrality condition,

$$N = \frac{4\pi}{3}(b^3 - a^3)N_d. \tag{3}$$

Penetration of the electron wave function into barrier is also neglected. In this case the potential outside dot does not depend on the space distribution of electron density inside the dot, and depends only on the total electrical charge of the dot. Therefore, outside the dot the electron potential energy is

$$V = V_0\left(\frac{1}{\xi} + \frac{\xi^2}{2} - \frac{3}{2}\right) \tag{4}$$

for $a \leqslant r \leqslant b$ and $V = 0$ for $r > b$,

$$V_0 = \frac{Ne^2}{\epsilon b(1 - (a/b)^3)}. \tag{5}$$

Here $\epsilon$ is the static dielectric permittivity and the dimensionless variable $\xi$ is $r/b$.

Considering $N$, $a$ and $N_d$ as adjustable parameters, we can find a structure with bound-to-continuum phototransitions shown in Fig. 2,

$$U_0 - E_F + V_m = hv, \tag{6}$$

where $V_m \equiv V(a)$ is the maximal barrier height. For example, for QDs made of $In_xGa_{1-x}As$ in $Al_yGa_{1-y}As$ matrix, with $x = 0.95$ and $y = 0.22$, the band-offset, $U_0$, is 220 meV. Using material

parameters $m = 0.067m_0$, $\epsilon = 12$, for $N_d = 10^{16}$ cm$^{-3}$, $N = 20$ and $a = 12$ nm, we found $E_F \approx 100$ meV, $V_m = 0.155$ meV, and $b = 78$ nm.

Consider a single QD as the center of the electron capture. We assume that the photoexcited electrons in a interdot region belong to continuous energy spectrum ($E > 0$). At room temperatures, for an electron with $m = 0.067m_0$ the de Broglie wavelength is $\sim$3 nm. The movement of such electron in a smooth potential between the QDs can be described by 3D momentum.

To be captured, the photoelectron should penetrate into the QD region, $r \leqslant a$. We will assume that the energy relaxation of this electron from the states ($E > 0$) to a final localized state in QD ($E < 0$) is provided by scattering with phonons. The electron can penetrate into the region $r \leqslant a$ due to thermoexcitation over the barrier or due to tunneling through the barrier (see Fig. 3). In order to compare the probabilities of these processes, we calculated the probability of tunneling, $\exp[-D(E)]$,

$$D = -\frac{2}{\hbar}\int_a^{r_0} \sqrt{2m(V - E)}\mathrm{d}r, \tag{7}$$

($r_0(E)$ is the turning point) and probability of thermoexcitation, $\exp[-(V_m - E)/kT]$.

The probability of tunneling and thermoexcitation along with relative probability of these processes are shown in Fig. 4. As seen, practically for all energies, up to $V_m$, thermoexcitation dominates over tunneling. Thus, the potential barriers very effectively prevent photoelectron capture. With barrier-limited capture the electron lifetime increases by the factor of $\exp(V_m/kT)$ in comparison with a flat-band structure. According to Eq. (1), the photoconductive gain also increases by the same factor. For typical parameters of the QD structure, such as $L = 1$ μm, $v_d = 10^6$ cm/s, and the capture time in the flat-band structure of 1–5 ps at 200 K, we get the photoconductive gain $\sim$100. Note, that according to Eq. (7), semiconductors with large effective mass are preferable. The high value of the gain allows one to improve detector characteristics.

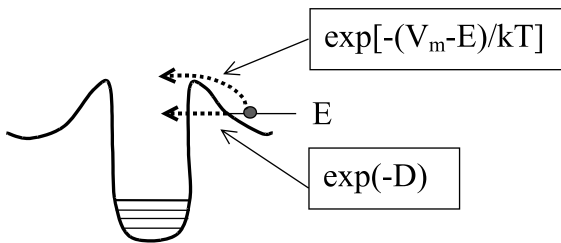


Fig. 3. Basic mechanism of photoelectron capture: tunneling and thermoexcitation.

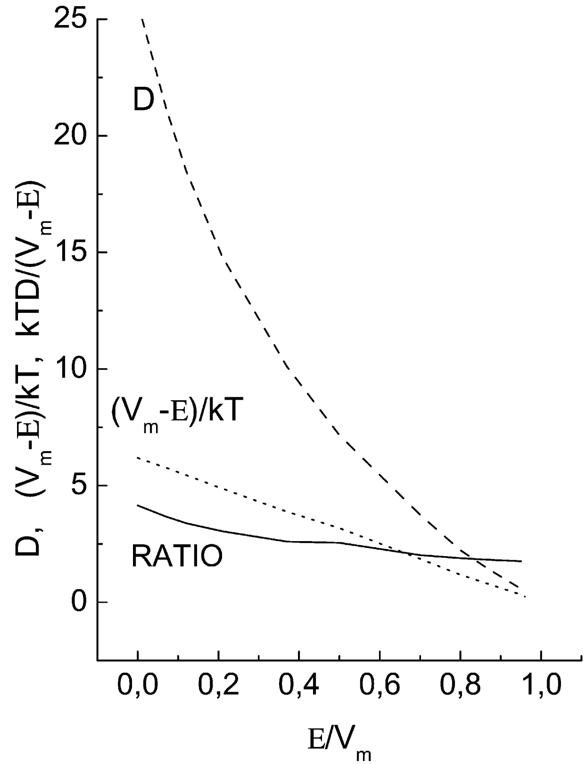


Fig. 4. Relative probability of tunneling and thermoexcitation.

## 3. Photodetector characteristics

As we discussed in previous sections, the incident infrared radiation generates bound-to-continuum electron transitions. The photocurrent, $I_p$, is given by

$$I_p = e\eta\Phi A, \tag{8}$$

where $\eta$ is the net quantum efficiency, $\Phi$ is the photon flux density (number of photons per sec-

ond per unit area), and $A$ is the photon illumination area. The photocurrent is proportional to the energy flux of the radiation, the corresponding coefficient, the responsivity, is

$$R = e\eta g/(h\nu), \tag{9}$$

where $\nu$ is the frequency of the incident electromagnetic radiation. The responsivity is directly proportional to the photoconductive gain. For suggested detector with barrier-limited electron capture we expect high responsivity, $R \sim 10^3\ \eta A/\mathrm{W}$ for 10 μm radiation. The high responsivity improves noise characteristics of the detector.

The noise equivalent power is defined as the noise power normalized by the square root of the frequency band. For a semiconducting photodetector, it may be written as

$$\mathrm{NEP} = [2eI_\mathrm{B} + 2egI_\mathrm{d} + 4kT/R_\mathrm{eq}]^{1/2}/R, \tag{10}$$

where $I_\mathrm{B}$ is the current due to background radiation, $R_\mathrm{eq}$ is the equivalent resistance of the external readout circuit and the detector resistor in parallel, $I_\mathrm{d}$ is the thermally generated dark current. The first term describes the fluctuations of background radiation. The second term is the generation–recombination (G–R) noise associated with random thermal excitations and decay of carriers (intrinsic noise). The third term is the Johnson noise caused by the random thermal motion of charge carries.

According to the Eq. (10), the Johnson noise is inversely proportional to the photoconductive gain. Therefore, in the suggested high-gain detector the Johnson noise is small. Note, that at low modulation frequency, the $1/f$ noise dominates over other noise mechanisms. The exact cause of $1/f$ noise is not known. Generally, this noise is aattributed to contacts or electrodes. It is important, that $1/f$ noise is also inversely proportional to the responsivity, and it will be small in the high-gain detector.

In the most useful mode of operation the thermal G–R noise should be slightly smaller than the noise of the background radiation. The G–R noise is independent on the photoconductive gain (in Eq. (10) the dark current is proportional to the gain), it may be also presented in the form

$$\mathrm{NEP}_\mathrm{G\text{–}R} = \frac{2h\nu}{\eta}\sqrt{\frac{N_\mathrm{th}}{\tau_1}}, \tag{11}$$

where $N_\mathrm{th}$ is the number of the thermally excited carries. Presence of barriers does not directly improve NEP, because the increase of the photocarrier lifetime is compensated by the increase of the thermally excited carries at low-energy levels (the levels with energy $\sim(h\nu - V_\mathrm{m})$ with respect to the Fermi level). However, the high gain allows one to reduce the detector volume, and to sacrifice the high responsivity in favor of the noise equivalent power.

## 4. Conclusions

We suggest a new design of infrared QD detector with potential barriers surrounding QDs. The barriers created by optimized interdot doping separate the localized electron ground state and the conducting states. The probability of tunneling of low-energy photoelectrons through the barriers is proportional to $\exp[-(e\beta/\hbar)(mNb/\epsilon)^{1/2}]$, $m$ is the effective mass, $N$ is the number of electrons in QD, $b$ is the size of the depletion area, $\beta \sim 1$. With appropriate parameters of the structure, it is possible to block tunneling of photoelectrons to QD. With barrier limited capture of photoelectrons, the electron lifetime and photoconductive gain increase by $\exp(V_\mathrm{m}/kT)$ factor ($V_\mathrm{m}$ is the height of the barrier) in comparison with the flat-band QD structure. The large photoconductive gain results in high responsivity, which in turn will improve detectivity and raise the device operating temperature.

## Acknowledgements

This work is supported by US ARO.

## References

[1] J.M. Arias, M. Zandian, J.G. Pasko, J. Bajaj, L.J. Kozlovski, W.E. Tennant, R.E. DeWames, MBE HgCdTe IRFPA flexible manufacturing, Proc. SPIE 2274 (1994) 2.

[2] P. Tribolet, J.P. Chatard, P. Costa, A. Manissadjian, Progress in HgCdTe homojunction infrared detectors, J. Cryst. Growth 184–185 (1998) 1262.

[3] B.F. Levine, Quantum-well infrared photodetectors, J. Appl. Phys. 74 (1993) R1.
[4] A. Rogalski, Comparison of the performance of quantum well and conventional bulk infrared photodetectors, Infrared Phys. Technol. 38 (1997) 295.
[5] L. Goldstein, F. Glas, J.Y. Marzin, M.N. Charasse, G. LeRoux, Growth by molecular beam epitaxy and characterization of InAs/GaAs strained-layer superlattices, Appl. Phys. Lett. 47 (1984) 1099.
[6] D. Leopard, M. Krishnamutthy, C.M. Reaves, S.P. Denbaars, P.M. Petroff, Direct formation of quantum-sized dots from uniform coherent islands of InGaAs on GaAs surfaces, Appl. Phys. Lett. 53 (1993) 3202.
[7] D. Pan, Y.P. Zeng, M.Y. Kong, J. Wu, C.H. Zhang, J.M. Li, C.Y. Wang, Normal incident infrared absorption from InGaAs/GaAs quantum dot superlattice, Electron. Lett. 32 (1996) 1726.
[8] J. Phillipse, K. Kamath, P. Bhattacharya, Far-infrared photoconductivity in self-organized InAs quantum dots, Appl. Phys. Lett. 72 (1998) 2020.
[9] J. Phillips, P. Bhattacharya, S.W. Kennerly, D.W. Beekman, M. Dutta, Self-assembled InAs–GaAs quantum-dot intersubband detectors, IEEE J. Quant. Electron. 35 (1999) 936.
[10] K.W. Berryman, S.A. Lyon, M. Segev, Mid-infrared photoconductivity in InAs quantum dots, Appl. Phys. Lett. 70 (1997) 1861.
[11] N. Horiguchi, T. Futatsugi, Y. Nataka, N. Yokoyama, T. Mankad, P.M. Petroff, Quantum dot infrared photodetector using modulation doped InAs self-assembled quantum dots, Jpn. J. Appl. Phys. 38 (1999) 2559.
[12] S.-W. Lee, K. Hirakawa, Y. Shimada, Bound-to-continuum interband photoconductivity of self-assembled InAs quantum dots in modulation-doped heterostructures, Appl. Phys. Lett. 75 (1999) 1428.
[13] U. Bockelmann, G. Bastard, Phonon scattering and energy relaxation in two-, one-, and zero-dimensional electron gases, Phys. Rev. B 42 (1990) 8947.
[14] D. Klotzkin, K. Kamath, P. Bhattacharya, Quantum capture times at room temperature in high-speed $In_{0.4}Ga_{0.6}As$–GaAs self-organized quantum-dot lasers, IEEE Photon. Technol. Lett. 9 (1997) 1301.
[15] D. Klotzkin, X. Zhang, P. Bhattacharya, R. Bhat, Carrier dynamics in high-speed multiquantum-well tunneling injection lasers determined from electrical impedance measurements, IEEE Photon. Technol. Lett. 9 (1997) 578.
[16] L. Chu, A. Zrenner, G. Bohn, G. Abstreiter, Normal-incident intersubband photocurrent spectroscopy on InAs/GaAs quantum dots, Appl. Phys. Lett. 75 (1999) 3599.
[17] V. Ryzhii, The theory of quantum-dot infrared phototransistors, Semicond. Sci. Technol. 11 (1996) 759.
[18] V. Ryzhii, M. Ershov, I. Khmyrova, M. Ryzhii, T. Iizuka, Multiple quantum dot infrared photodetectors, Phys. B 227 (1996) 17.
[19] S.J. Xu, S.J. Chua, T. Mei, X.C. Wang, X.H. Zhang, G. Karunasiri, W.J. Fan, C.H. Wang, J. Jiang, S. Wang, X.G. Xie, Characteristics of InGaAs quantum dot infrared photodetectors, Appl. Phys. Lett. 73 (1998) 3153.